

This is a repository copy of *Transcription factors in eukaryotic cells can functionally regulate gene expression by acting in oligomeric assemblies formed from an intrinsically disordered protein phase transition enabled by molecular crowding.*

White Rose Research Online URL for this paper:

<https://eprints.whiterose.ac.uk/130472/>

Version: Accepted Version

---

**Article:**

Leake, Mark Christian orcid.org/0000-0002-1715-1249 (2018) Transcription factors in eukaryotic cells can functionally regulate gene expression by acting in oligomeric assemblies formed from an intrinsically disordered protein phase transition enabled by molecular crowding. *Transcription*. pp. 298-306.

<https://doi.org/10.1080/21541264.2018.1475806>

---

**Reuse**

This article is distributed under the terms of the Creative Commons Attribution (CC BY) licence. This licence allows you to distribute, remix, tweak, and build upon the work, even commercially, as long as you credit the authors for the original work. More information and the full terms of the licence here:

<https://creativecommons.org/licenses/>

**Takedown**

If you consider content in White Rose Research Online to be in breach of UK law, please notify us by emailing [eprints@whiterose.ac.uk](mailto:eprints@whiterose.ac.uk) including the URL of the record and the reason for the withdrawal request.

# Transcription

Transcription factors in eukaryotic cells can functionally regulate gene expression by acting in oligomeric assemblies formed from an intrinsically disordered protein phase transition enabled by molecular crowding

--Manuscript Draft--

<b>Manuscript Number:</b>	KTRN-2018-0012R1
<b>Article Type:</b>	Point-of-View
<b>Keywords:</b>	gene expression; transcription factors; single-molecule; super-resolution; cell signaling; intrinsically disordered protein; phase transition; molecular crowding; fluorescent protein
<b>Corresponding Author:</b>	Mark Leake  UNITED KINGDOM
<b>First Author:</b>	Mark Leake
<b>Order of Authors:</b>	Mark Leake
<b>Manuscript Region of Origin:</b>	UNITED KINGDOM
<b>Abstract:</b>	High-speed single-molecule fluorescence microscopy in vivo shows that transcription factors in eukaryotes can act in oligomeric clusters mediated by molecular crowding and intrinsically disordered protein. This finding impacts on the longstanding puzzle of how transcription factors find their gene targets so efficiently in the complex, heterogeneous environment of the cell.



## 19 **Abstract**

20 High-speed single-molecule fluorescence microscopy in vivo shows that transcription factors  
21 in eukaryotes can act in oligomeric clusters mediated by molecular crowding and intrinsically  
22 disordered protein. This finding impacts on the longstanding puzzle of how transcription  
23 factors find their gene targets so efficiently in the complex, heterogeneous environment of the  
24 cell.

## 25 **Introduction**

26  
27 Cells regulate gene expression through binding of transcription factors (TFs) to promoters to  
28 turn gene expression on or off (1, 2). Simulations show that the time it takes for TFs to find  
29 their targets through pure 3D diffusion alone is ~six orders of magnitude larger than what is  
30 observed experimentally (3). Hypotheses to explain this observation have included TF  
31 heterogeneous mobility comprising a combination of free 3D diffusion combined with sliding  
32 and hopping on the DNA plus longer jumps between different DNA strands called  
33 intersegment transfer (4–6). In eukaryotic cells, TF localization fluctuates, often between  
34 cytoplasm and nucleus (7). Although it has been observed that promoters can pool on the  
35 genome in clusters (8) it has not previously been seen that TFs themselves act in clusters, but  
36 instead are largely assumed to act as single molecules. Simulations which embody diffusion  
37 and binding suggest that multivalent TFs could, in principle, facilitate intersegment transfer  
38 (9). Previously, single-molecule fluorescence microscopy has been used to study TF  
39 localization in living cells across a range of model organisms, including bacteria, yeast and  
40 multi-cellular organisms (10–16). Many studies suggest complexities in diffusion and binding  
41 (4, 12, 15, 17, 18) which may include intersegmental transfer (4, 17, 18). However, until now,  
42 the direct experimental evidence for intersegmental transfer has been limited.

43 Many of the important features of gene expression control in eukaryotes are  
44 exemplified in the model unicellular microorganism *Saccharomyces cerevisiae* (budding  
45 yeast). In particular, its glucose sensing pathway presents an experimentally tractable system  
46 to study gene regulation. Here, control of gene expression is achieved by TFs which include  
47 the Zn finger DNA binding protein Mig1 (19) that acts to repress expression from targets  
48 including *GAL* genes involved in glucose metabolism (20). Mig1 localizes towards the  
49 nucleus if the extracellular glucose concentration is increased (21), correlated to its own  
50 dephosphorylation by a protein called Snf1 (22, 23).

51 In recent investigations from my own group (24) the spatiotemporal dynamics and  
52 kinetics of gene regulation in live *S. cerevisiae* cells, using its glucose sensing pathway as a  
53 model for signal transduction, was explored using physics methods which enable the  
54 understanding of the processes of life one molecule at a time (25, 26), employing ‘single-  
55 molecule optical proteomics’ tools (27). The combination of these advanced light microscopy  
56 with genetics techniques has previously enabled valuable insights into the activities of several  
57 other processes for low copy number proteins (28) in both unicellular organisms and single  
58 cells from more complex multicellular organisms (29). These single-molecule/cell and super-  
59 resolution microscopy tools have in particular been applied to integrated membrane proteins  
60 (30, 31), such as interaction networks like oxidative phosphorylation (32–36), cell division  
61 processes (37–39) and protein translocation (40), along with bacterial cell motility (41–44).  
62 The tools can also probe the aqueous environment of cells as opposed to just on their  
63 hydrophobic cell membrane surface, including processes of DNA  
64 replication/remodeling/repair (45–47), and systems more directly relevant to biomedicine  
65 such as bacterial infection (48–50).

66 In this Points of View article I discuss further the findings from my team from single-  
67 molecule fluorescence microscopy to track functional TFs with very high speed to match

68 typical rates of protein diffusion in live cells and thereby enable ‘blur-free’ observations. We  
69 were able to quantify the composition and dynamics of Mig1 under normal and perturbed  
70 conditions which affected its state of phosphorylation, and also performed experiments on a  
71 protein called Msn2 which functions antagonistically, i.e. instead as an enhancer/activator,  
72 for many of the same Mig1 target genes (51) through a completely different signaling  
73 pathway. The results showed unexpectedly that Mig1 binds to its target genes as an  
74 oligomeric cluster which has stoichiometries in the range ~6-9 molecules. We found evidence  
75 that Mig1 molecules in a cluster are glued together through interactions of intrinsically  
76 disordered peptide sequences innervated by molecular crowding depletion forces in the cell.  
77 Our findings may reveal a more general eukaryotic cell strategy for the control of gene  
78 expression which uses intrinsic disorder of many TFs to form clusters that then enable large  
79 reductions in the time taken to find a given target gene.

80

## 81 **Results**

### 82 **Single-molecule optical proteomics indicates the presence of Mig1 oligomeric clusters**

83 We used millisecond Slimfield single-molecule fluorescence imaging (46, 52, 53) on live *S.*  
84 *cerevisiae* cells (Fig. 1A) using a green fluorescent protein (GFP) reporter for Mig1  
85 integrated into the genome, including mCherry reporter on the RNA polymerase subunit  
86 protein Nrd1 to indicate the position of the cell nucleus. Slimfield was optimized for single-  
87 molecule detection sensitivity by using an *in vitro* imaging assay (54). We also measured the  
88 maturation effect of the fluorescent proteins in these cells (55) and estimate it to be <15%  
89 immature fluorescent protein over the timescale of imaging experiments. Note, Slimfield  
90 limits the observation area to an equivalent diameter of <10  $\mu\text{m}$  in the lateral plane to achieve  
91 rapid imaging sample times of millisecond and, in some instances sub-millisecond levels  
92 (56), but is less ideal to eukaryotic imaging of cells with larger nuclei. A host of other  
93 single-molecule techniques based on light-sheet imaging have larger fields of view, and also  
94 combine low background and low light toxicity. For the interested reader, these include:  
95 HILO (by Tokunaga M.N. et al. (57)), AFM cantilever lightsheet (by Gebhardt, J.C. et al.  
96 (11)), lattice light-sheet (by Chen B.C. et al. (58)), multi-focus (by Abrahamsson S. et  
97 al.(59)), remote focusing (by Yang et al.(60)), and diagonally scanned light sheet (by Dean et  
98 al.(61)).

99 Under depleted /elevated extracellular *glucose* (-/+ ) we measured cytoplasmic and  
100 nuclear Mig1 localization bias respectively, visible in individual cells by our generating rapid  
101 microfluidic exchange (a few seconds) of extracellular fluid (Fig. 1B), and resolved two  
102 components under both conditions consistent with a diffuse monomeric pool and distinct  
103 oligomeric foci of Mig1 (Fig. 1C). The foci were also visible as hotspots using the green-red  
104 photoswitchable fluorescent protein mEos2 (62) excited by super-resolution stochastic optical  
105 reconstruction microscopy (STORM) (Fig. 1C), with modeling using 3C structural data of the  
106 yeast chromosome (63) and sequence alignment analysis for the location of Mig1 target  
107 promoters supporting the hypothesis that the majority of Mig1 clusters were specifically  
108 binding to Mig1 target genes.

109 Nanoscale tracking determined the position of tracked Mig1 foci to a lateral precision  
110 of 40 nm (33, 64) coupled to stoichiometry analysis using stepwise photobleaching of GFP  
111 (54) and single cell copy number analysis (65). An additional output from the tracking was  
112 the effective diffusion coefficient  $D$  as a function of its location in either the cytoplasm,  
113 nucleus or translocating across the nuclear envelope, as well as the copy number of Mig1  
114 molecules associated with each subcellular region and in each cell as a whole, indicating  
115 ~850-1,300 Mig1 molecules per cell dependent on extracellular glucose. It should be noted

116 that confinement may affect the apparent diffusion coefficient in the small volume of a yeast  
117 nucleus if the length the mean square displacement (MSD) of tracked particles is comparable  
118 to the diameter of the nucleus, however, if our case only the short length scale MSD regions  
119 are considered to determine  $D$ .

120 In control experiments, a modified strain (51) generated with a binding site for protein  
121 PP7 on mRNA produced by one of the Mig1 target genes called *GSY1* showed colocalization  
122 between PP7-GFP expressed off a plasmid and Mig1-mCherry expressed genomically under  
123 high glucose conditions. We also observed similar clustering and co-localization to PP7 for  
124 the antagonistic TF Msn2. These PP7 co-localization results suggest that clusters both of  
125 Mig1 and Msn2 are *functionally* active in regulating target gene expression of the test target  
126 gene *GSY1*.

127

### 128 **Cytoplasmic Mig1 diffuses rapidly but nuclear Mig1 can be mobile and immobile**

129 Cytoplasmic Mig1 fluorescent foci at *glucose* (+/-), and nuclear foci at *glucose* (-), were  
130 consistent with just a single mobile population whose  $D$  of  $1-2 \mu\text{m}^2/\text{s}$  consistent with earlier  
131 observations. However, nuclear foci at *glucose* (+) indicated a mixture of mobile and  
132 immobile components (Fig. 1D). These results suggested 20-30% of nuclear foci are  
133 immobile, consistent with a DNA-bound state. MSD analysis of foci tracks indicated  
134 Brownian diffusion over a few tens of ms but increasingly anomalous diffusion over longer  
135 timescales, consistent with *glucose* (+) Mig1 diffusion being impacted by interactions with  
136 nuclear structures, similar to that reported for other TFs (66). Here, this interaction depended  
137 on extracellular glucose despite Mig1 requiring a pathway of proteins to detect it, unlike the  
138 more direct detection mechanism of the prokaryotic *lac* repressor. Control experiments with  
139 Zn finger deletion strains of Mig1 indicated that Mig1 clusters bind to the DNA via their Zn  
140 finger motif with direct glucose dependence. At the high laser excitation intensities used for  
141 Slimfield imaging photobleaching is rapid, and so typically a single GFP molecule will  
142 photobleach on average after 5-10 consecutive image frame. To account for this we  
143 interpolate observed foci brightness values back to the start of each photobleach using an  
144 exponential photobleach function. We observed no direct evidence for irreversible  
145 photobleaching (i.e. 'photoblinking') with GFP at these intensities, though other fluorescent  
146 proteins such as YFP have been known to exhibit such blinking behavior, which if so would  
147 need to be further characterized, for example using surface immobilized purified YFP *in*  
148 *vitro* samples. A general compromise here, however, is to confine tracking analysis to  
149 typically less than 100 ms of laser exposure so that irreversible photoblinking is more  
150 dominant than reversible blinking.

151

152

### 153 **Mig1 nuclear pore complex selectivity is mediated by interactions distant from the** 154 **nuclear envelope**

155 We compared the spatiotemporal dynamics of different Mig1 clusters during translocation by  
156 converting trans-nuclear tracks into coordinates parallel and perpendicular to the measured  
157 nuclear envelope location, and synchronizing coordinate origins to be at the nuclear envelope  
158 crossing point for a given foci track. A heat map of spatial locations of translocating clusters  
159 indicated a hotspot of comparable volume to the nuclear pore complexes and accessory  
160 structures (67, 68) (Fig. 1E). The dwell time during nuclear envelope translocation was  
161  $\sim 10$  ms, similar to previous estimates for transport factors (69) but here found to be  
162 insensitive to glucose (Fig. 1F), demonstrating that there is no direct selectivity on the basis

163 of TF phosphorylation state by nuclear pore complexes themselves which suggests that cargo  
164 selectivity mechanisms of nuclear transport (70) are blind to phosphorylation state. Coupled  
165 with the observation that Mig1 at *glucose* (-) does not exhibit immobility in the nucleus and  
166 that Mig1 lacking the Zn finger still accumulates in the nucleus at *glucose* (+) this suggests  
167 that Mig1 localization is driven by changes in Mig1 binding affinity to other proteins, e.g.  
168 the general co-repressor complex at the genome (71), or outside the nucleus not involving the  
169 nuclear pore complex.

170

### 171 **Mig1 nuclear clusters turn over in >100 s**

172 By modifying the microscope we were able to implement fluorescence recovery after  
173 photobleaching (FRAP) to probe nuclear turnover of Mig1, by focusing a separate laser onto  
174 just the nucleus, photobleaching this region with a rapid 200 ms pulse, and quantifying any  
175 subsequent fluorescence intensity recovery into that region (Fig. 1G). We could then acquire  
176 images with millisecond precision for individual frames but stroboscopically illuminating to  
177 extend the range of time scales for recovery before significant GFP photobleaching occurred,  
178 enabling FRAP observations at a single-molecule precision to timescales >1,000 s. Analyses  
179 demonstrated measurable recovery for both foci and the diffuse pool components in the  
180 nucleus, which could be fitted by single exponential functions indicating fast recovery of pool  
181 at both *glucose* (-) and (+) with a time constant of just a few seconds but a larger time  
182 constant at *glucose* (+) for nuclear foci of at least ~100s (Fig. 1H), with recovery of intensity  
183 being consistent with units of ~7-9 GFP molecules for the foci component but no obvious  
184 periodicity in stoichiometry measurable from pool recovery. These data suggested that  
185 molecular turnover at nuclear foci of Mig1 bound to target genes occurred in units of whole  
186 Mig1 clusters.

187

### 188 **Clusters are stabilized by molecular crowding and intrinsic disorder**

189 Native, denaturing gel electrophoresis and western blots on purified extracts from Mig1-GFP  
190 cells (Fig. 1I) indicated a single band corresponding to Mig1. *In vitro* Slimfield imaging of  
191 purified Mig1-GFP under identical imaging conditions for live cells similarly indicated  
192 monomeric Mig1-GFP foci in addition to a small fraction of brighter foci which were  
193 consistent with chance overlap of monomer GFP images. However, addition of a molecular  
194 crowding reagent in the form of low molecular weight polyethylene glycol (PEG) at a  
195 concentration known to correspond to small molecule 'depletion' forces in cells (72) resulted  
196 in significant numbers of oligomers (Fig. 1J), suggesting that Mig1 clusters present in live  
197 cells regardless of glucose may be stabilized by depletion components that are lost during  
198 biochemical purification.

199 Secondary structure predictions suggested significant regions of disorder away from  
200 the Zn finger binding motif. We measured changes in circular dichroism of the Mig1 fusion  
201 construct upon addition of PEG (Fig. 1K) in a wavelength range known to be sensitive to  
202 transitions between ordered and intrinsically disordered states (73, 74). We also noted similar  
203 levels of disorder content in the Msn2 protein far from the Zn finger motif. These  
204 observations suggested a TF 'molecular bipolarity', in regards to disorder content, which  
205 stabilizes a cluster compact core focused around the disordered regions that undergo a  
206 putative phase transition to a more structure state, while exposing Zn fingers and positive  
207 surface charges to enable specific and non-specific interactions with accessible DNA strands  
208 (Fig. 1L).

## 210 **Perspective**

211 Our findings address aspects of functional gene regulation in live cells which have hitherto  
212 been unexplored, using biophysical technology that has not been available until recently. The  
213 results strongly support a functional link between Mig1 and Msn2 TF clusters and target gene  
214 expression; a biological role of multivalent TFs for enhancing intersegmental transfer had  
215 been elucidated previously in simulations (9) but unobserved experimentally until our  
216 discoveries here, and so our findings impact on the longstanding question of how TFs might  
217 find their targets in the genome so efficiently. Clustering of a range of nuclear factors has  
218 been observed previously using single-molecule techniques, such as transient RNA  
219 Polymerase II cluster dynamics in living cells using time-correlated PALM (tc-PALM) (75,  
220 76). Also functional nuclear protein clusters have been seen (77) and the Bicoid transcription  
221 factor in fruit fly embryos has been observed to form clusters mediated in part mediated by  
222 intrinsically disordered peptide sequences (78).

223         Quantifying nearest-neighbor distances between Mig1 promoter sites in the *S.*  
224 *cerevisiae* genome from the 3C model indicates 20-30% are <50 nm apart, small enough to  
225 enable different DNA segments to be linked though intersegment transfer by a single cluster  
226 (6, 9), which would also enable in principle simultaneous binding of >1 gene target from just  
227 a single TF cluster. There is a net positive charge in the vicinity of Zn finger motifs, and this  
228 would also enable non-specific electrostatic interactions with the negatively charged  
229 phosphate backbone of DNA, facilitating 1D sliding diffusion of the protein along a DNA  
230 strand. Thus, a cluster may be able to slide along DNA in a largely sequence-independent  
231 manner and undergo intersegmental transfer to a neighboring strand relatively easily, either  
232 spontaneously or stimulated by the presence of protein barriers on the DNA in a process  
233 likely to have some sequence dependence when an obstacle is encountered. In particular,  
234 bound RNA polymerases present during gene transcription at sequence specific sites could  
235 act as roadblocks to kick off translocating clusters from a DNA strand, to again facilitate  
236 intersegmental transfer and thus increase the ultimate chances that TF clusters will encounter  
237 one of the gene targets and specifically bind via the Zn finger motif, thus predominantly  
238 circumventing the requirement for significant amounts of slow 3D diffusion in the  
239 nucleoplasm.

240         Our discovery is, to our knowledge, the first to make a link between predicted disorder  
241 and the ability to form oligomeric clusters in TFs. Our findings may potentially offer some  
242 insights into addressing the longstanding question of why in general there is so much  
243 predicted disorder in eukaryote transcription factors; ~90% of eukaryotic TFs indicate  
244 significant proportions of sequences with disordered content (79). Our finding that protein  
245 interactions based on relatively weak molecular crowding depletion forces has functional  
246 relevance in several areas of cell biology, such as processes involving aggregation mediated  
247 through intrinsic disorder interactions; for example, those of amyloid plaques found in  
248 neurodegenerative disorders including Alzheimer's and Parkinson's diseases (80). Increased  
249 understanding of the clustering mechanism might therefore be of value in understanding the  
250 progression of these diseases. Open questions remain though: for example, are clusters homo-  
251 oligomeric or do they contain multiple different TFs? How is specificity maintained inside a  
252 cluster? Are the components of the clusters themselves dynamic and undergo molecular  
253 turnover? Can the ability to cluster be controlled, for example by switching the state of  
254 phosphorylation?  
255

## 256 **Acknowledgments**



257 The work of the original research article described (24) also involved Adam Wollman,  
258 Sviatlana Shashkova, Erik Hedlund, Rosemarie Friemann and Stefan Hohmann, and the  
259 Bioscience Technology Facility of the University of York, UK. Thanks to Mark Johnston  
260 (CU Denver) for a Mig1 phosphorylation mutant plasmid, and Michael Elowitz (Caltech) for  
261 a Mig1/Msn2/PP7 and Zn finger deletion strain.

262

## 263 **Funding**

264 Supported by the Biological Physical Sciences Institute, Royal Society, MRC (grant  
265 MR/K01580X/1), BBSRC (grant BB/N006453/1), Swedish Research Council and European  
266 Commission via Marie Curie-Network for Initial training ISOLATE (Grant agreement nr:  
267 289995) and the Marie Curie Alumni Association.

268

## 269 **Conflict of interest**

270 There are no conflicts of interests.

271

## 272 **References**

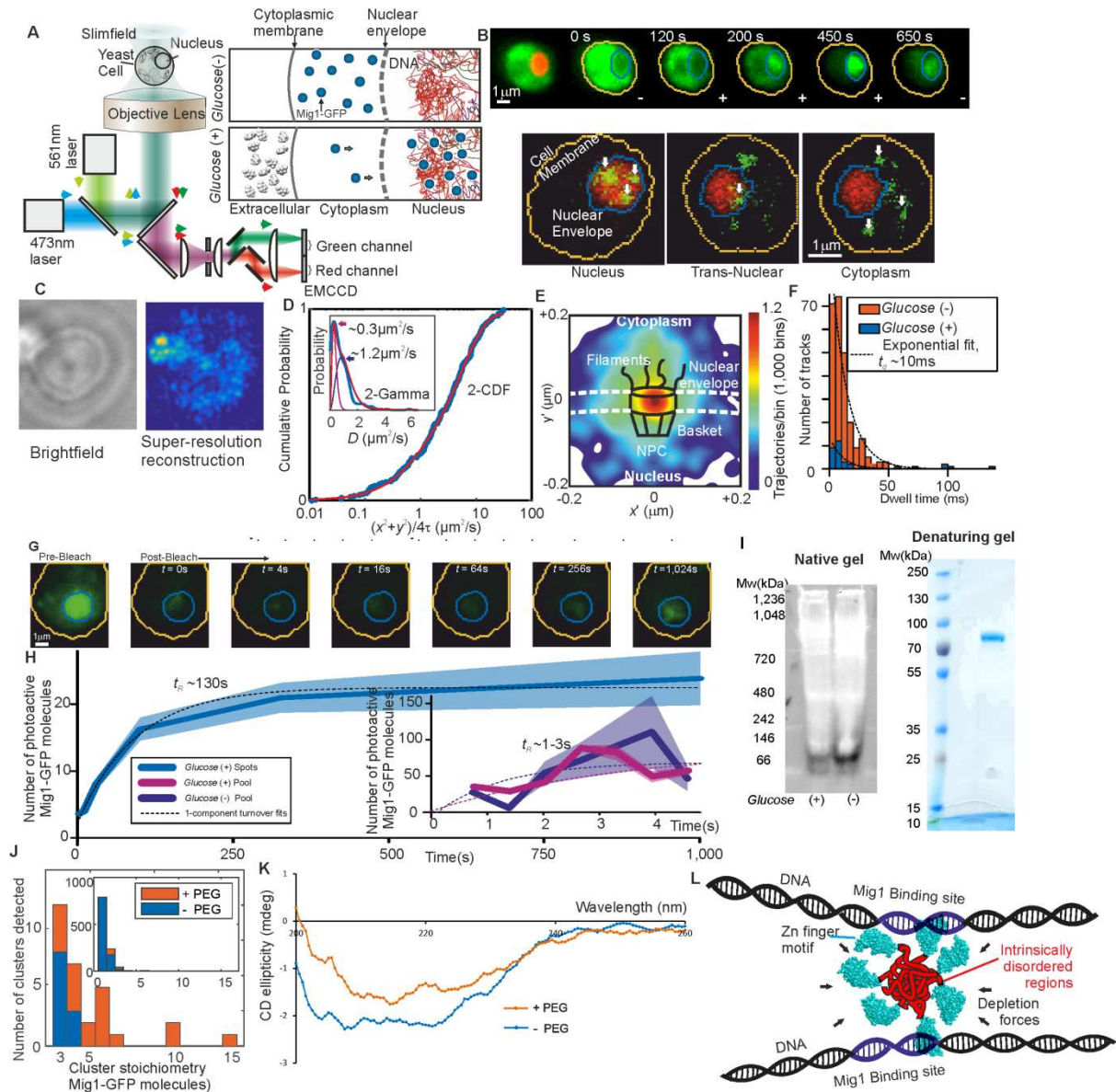
- 273 1. F. Jacob, J. Monod, Genetic regulatory mechanisms in the synthesis of proteins. *J.*  
274 *Mol. Biol.* **3**, 318–356 (1961).
- 275 2. J. Gertz, E. D. Siggia, B. A. Cohen, Analysis of combinatorial cis-regulation in  
276 synthetic and genomic promoters. *Nature.* **457**, 215–8 (2009).
- 277 3. O. G. Berg, R. B. Winter, P. H. Von Hippel, Diffusion-driven mechanisms of protein  
278 translocation on nucleic acids. 1. Models and theory. *Biochemistry.* **20**, 6929–6948  
279 (1981).
- 280 4. A. Mahmutovic, O. G. Berg, J. Elf, What matters for lac repressor search in vivo--  
281 sliding, hopping, intersegment transfer, crowding on DNA or recognition? *Nucleic*  
282 *Acids Res.* **43**, 3454–64 (2015).
- 283 5. S. E. Halford, J. F. Marko, How do site-specific DNA-binding proteins find their  
284 targets? *Nucleic Acids Res.* **32**, 3040–52 (2004).
- 285 6. D. M. Gowers, S. E. Halford, Protein motion from non-specific to specific DNA by  
286 three-dimensional routes aided by supercoiling. *EMBO J.* **22**, 1410–8 (2003).
- 287 7. S. T. Whiteside, S. Goodbourn, Signal transduction and nuclear targeting: regulation of  
288 transcription factor activity by subcellular localisation. *J. Cell Sci.* **104** ( Pt 4, 949–55  
289 (1993).
- 290 8. C. T. Harbison *et al.*, Transcriptional regulatory code of a eukaryotic genome. *Nature.*  
291 **431**, 99–104 (2004).
- 292 9. H. G. Schmidt, S. Sewitz, S. S. Andrews, K. Lipkow, An Integrated Model of  
293 Transcription Factor Diffusion Shows the Importance of Intersegmental Transfer and  
294 Quaternary Protein Structure for Target Site Finding. **9**, e108575 (2014).
- 295 10. G.-W. Li, X. S. Xie, Central dogma at the single-molecule level in living cells. *Nature.*  
296 **475**, 308–15 (2011).
- 297 11. J. C. M. Gebhardt *et al.*, Single-molecule imaging of transcription factor binding to  
298 DNA in live mammalian cells. *Nat. Methods.* **10**, 421–426 (2013).

- 299 12. D. Normanno *et al.*, Probing the target search of DNA-binding proteins in mammalian  
300 cells using TetR as model searcher. *Nat. Commun.* **6**, 7357 (2015).
- 301 13. D. Mazza, A. Abernathy, N. Golob, T. Morisaki, J. G. McNally, A benchmark for  
302 chromatin binding measurements in live cells. *Nucleic Acids Res.* **40**, e119 (2012).
- 303 14. Z. Liu *et al.*, 3D imaging of Sox2 enhancer clusters in embryonic stem cells. *Elife.* **3**,  
304 e04236 (2014).
- 305 15. J. Chen *et al.*, Single-Molecule Dynamics of Enhanceosome Assembly in Embryonic  
306 Stem Cells. *Cell.* **156**, 1274–1285 (2014).
- 307 16. Z. Zhang *et al.*, Rapid dynamics of general transcription factor TFIIB binding during  
308 preinitiation complex assembly revealed by single-molecule analysis. *Genes Dev.* **30**,  
309 2106–2118 (2016).
- 310 17. P. Hammar *et al.*, The lac repressor displays facilitated diffusion in living cells.  
311 *Science.* **336**, 1595–8 (2012).
- 312 18. J. C. M. Gebhardt *et al.*, Single-molecule imaging of transcription factor binding to  
313 DNA in live mammalian cells. *Nat. Methods.* **10**, 421–6 (2013).
- 314 19. J. O. Nehlin, M. Carlberg, H. Ronne, Control of yeast GAL genes by MIG1 repressor:  
315 a transcriptional cascade in the glucose response. *EMBO J.* **10**, 3373–7 (1991).
- 316 20. E. Frolova, Binding of the glucose-dependent Mig1p repressor to the GAL1 and GAL4  
317 promoters in vivo: regulation by glucose and chromatin structure. *Nucleic Acids Res.*  
318 **27**, 1350–1358 (1999).
- 319 21. M. J. De Vit, J. a Waddle, M. Johnston, Regulated nuclear translocation of the Mig1  
320 glucose repressor. *Mol. Biol. Cell.* **8**, 1603–18 (1997).
- 321 22. L. Bendrioua *et al.*, Yeast AMP-activated Protein Kinase Monitors Glucose  
322 Concentration Changes and Absolute Glucose Levels. *J. Biol. Chem.* **289**, 12863–75  
323 (2014).
- 324 23. S. Shashkova, A. J. M. Wollman, M. C. Leake, S. Hohmann, The yeast Mig1  
325 transcriptional repressor is dephosphorylated by glucose-dependent and -independent  
326 mechanisms. *FEMS Microbiol. Lett.* **364** (2017), doi:10.1093/femsle/fnx133.
- 327 24. A. J. M. J. Wollman *et al.*, Transcription factor clusters regulate genes in eukaryotic  
328 cells. **6**, e27451 (2017).
- 329 25. M. C. Leake, The physics of life: one molecule at a time. *Philos. Trans. R. Soc. Lond.*  
330 *B. Biol. Sci.* **368**, 20120248 (2013).
- 331 26. H. Miller, Z. Zhou, J. Shepherd, A. J. M. Wollman, M. C. Leake, Single-molecule  
332 techniques in biophysics: a review of the progress in methods and applications.  
333 *Reports Prog. Phys.* **81**, 24601 (2018).
- 334 27. S. Shashkova, M. C. Leake, Single-molecule fluorescence microscopy review:  
335 Shedding new light on old problems. *Biosci. Rep.* **37** (2017),  
336 doi:10.1042/BSR20170031.
- 337 28. B. Huang *et al.*, Counting Low-Copy Number Proteins in a Single Cell. *Science.* **315**,  
338 81–4 (2007).
- 339 29. M. Wu, A. K. Singh, Single-cell protein analysis. *Curr. Opin. Biotechnol.* **23**, 83–8  
340 (2012).

- 341 30. S. J. Bryan *et al.*, Localisation and interactions of the Vipp1 protein in cyanobacteria.  
342 *Mol. Microbiol.* **94**, 1179–1195 (2014).
- 343 31. A. Nenner *et al.*, Independent mobility of proteins and lipids in the plasma  
344 membrane of *Escherichia coli*. *Mol. Microbiol.* **92**, 1142–53 (2014).
- 345 32. T. Lenn, M. C. Leake, Single-molecule studies of the dynamics and interactions of  
346 bacterial OXPHOS complexes. *Biochim. Biophys. Acta - Bioenerg.* **1857**, 224–231  
347 (2016).
- 348 33. I. Llorente-Garcia *et al.*, Single-molecule in vivo imaging of bacterial respiratory  
349 complexes indicates delocalized oxidative phosphorylation. *Biochim. Biophys. Acta.*  
350 **1837**, 811–24 (2014).
- 351 34. Y. T. Lenn, M. C. Leake, C. W. Mullineaux, Are *Escherichia coli* OXPHOS  
352 complexes concentrated in specialized zones within the plasma membrane? *Biochem.*  
353 *Soc. Trans.* **36**, 1032–6 (2008).
- 354 35. T. Lenn, M. C. Leake, C. W. Mullineaux, Clustering and dynamics of cytochrome bd-I  
355 complexes in the *Escherichia coli* plasma membrane in vivo. *Mol. Microbiol.* **70**,  
356 1397–407 (2008).
- 357 36. A. Badrinarayanan, M. C. Leake, Using Fluorescence Recovery After Photobleaching  
358 (FRAP) to Study Dynamics of the Structural Maintenance of Chromosome (SMC)  
359 Complex In Vivo. *Methods Mol. Biol.* **1431**, 37–46 (2016).
- 360 37. S.-W. S.-W. Chiu, M. A. J. Roberts, M. C. Leake, J. P. Armitage, Positioning of  
361 chemosensory proteins and ftsz through the *Rhodobacter sphaeroides* cell cycle. *Mol.*  
362 *Microbiol.* **90**, 322–37 (2013).
- 363 38. A. W. Bisson-Filho *et al.*, Treadmilling by FtsZ filaments drives peptidoglycan  
364 synthesis and bacterial cell division. *Science.* **355**, 739–743 (2017).
- 365 39. V. A. Lund *et al.*, Molecular coordination of *Staphylococcus aureus* cell division.  
366 *Elife.* **7**, e32057 (2018).
- 367 40. M. C. Leake *et al.*, Variable stoichiometry of the TatA component of the twin-arginine  
368 protein transport system observed by in vivo single-molecule imaging. *Proc. Natl.*  
369 *Acad. Sci. U. S. A.* **105**, 15376–81 (2008).
- 370 41. S. W. W. Reid *et al.*, The maximum number of torque-generating units in the flagellar  
371 motor of *Escherichia coli* is at least 11. *Proc. Natl. Acad. Sci. U. S. A.* **103**, 8066–71  
372 (2006).
- 373 42. Y. Sowa *et al.*, Direct observation of steps in rotation of the bacterial flagellar motor.  
374 *Nature.* **437**, 916–9 (2005).
- 375 43. T. Pilizota *et al.*, A molecular brake, not a clutch, stops the *Rhodobacter sphaeroides*  
376 flagellar motor. *Proc. Natl. Acad. Sci. U. S. A.* **106**, 11582–7 (2009).
- 377 44. C.-J. Lo, M. C. Leake, T. Pilizota, R. M. Berry, Nonequivalence of membrane voltage  
378 and ion-gradient as driving forces for the bacterial flagellar motor at low load.  
379 *Biophys. J.* **93**, 294–302 (2007).
- 380 45. R. Reyes-Lamothe, D. J. Sherratt, M. C. Leake, Stoichiometry and architecture of  
381 active DNA replication machinery in *Escherichia coli*. *Science.* **328**, 498–501 (2010).
- 382 46. A. Badrinarayanan, R. Reyes-Lamothe, S. Uphoff, M. C. Leake, D. J. Sherratt, In vivo  
383 architecture and action of bacterial structural maintenance of chromosome proteins.

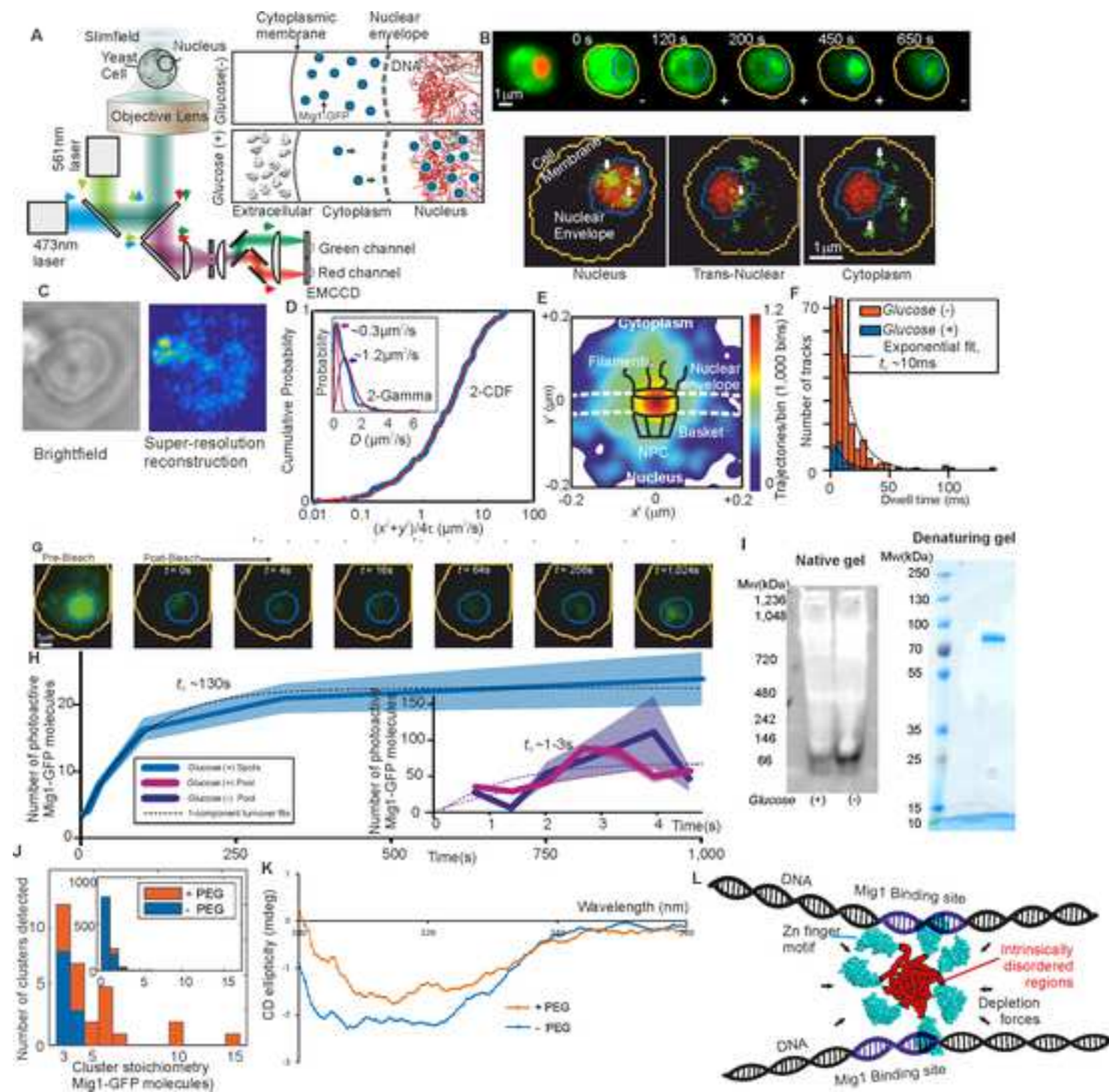
- 384 *Science*. **338**, 528–31 (2012).
- 385 47. A. J. M. Wollman, A. H. Syeda, P. McGlynn, M. C. Leake, Single-molecule  
386 observation of DNA replication repair pathways in *E. coli*. *Adv. Exp. Med. Biol.* **915**,  
387 5–16 (2016).
- 388 48. M. C. Leake, The Biophysics of Infection. *Adv. Exp. Med. Biol.* **915**, 1–3 (2016).
- 389 49. H. Miller, A. J. M. Wollman, M. C. Leake, Designing a Single-Molecule Biophysics  
390 Tool for Characterising DNA Damage for Techniques that Kill Infectious Pathogens  
391 Through DNA Damage Effects. *Adv. Exp. Med. Biol.* **915**, 115–27 (2016).
- 392 50. A. J. M. Wollman, H. Miller, S. Foster, M. C. Leake, An automated image analysis  
393 framework for segmentation and division plane detection of single live *Staphylococcus*  
394 *aureus* cells which can operate at millisecond sampling time scales using bespoke  
395 Slimfield microscopy. *Phys. Biol.* **5**, 55002 (2016).
- 396 51. Y. Lin, C. H. Sohn, C. K. Dalal, L. Cai, M. B. Elowitz, Combinatorial gene regulation  
397 by modulation of relative pulse timing. *Nature*. **527**, 54–58 (2015).
- 398 52. M. Plank, G. H. Wadhams, M. C. Leake, Millisecond timescale slimfield imaging and  
399 automated quantification of single fluorescent protein molecules for use in probing  
400 complex biological processes. *Integr. Biol. (Camb)*. **1**, 602–12 (2009).
- 401 53. R. Reyes-Lamothe, D. J. Sherratt, M. C. Leake, Stoichiometry and architecture of  
402 active DNA replication machinery in *Escherichia coli*. *Science*. **328**, 498–501 (2010).
- 403 54. M. C. Leake *et al.*, Stoichiometry and turnover in single, functioning membrane  
404 protein complexes. *Nature*. **443**, 355–358 (2006).
- 405 55. S. Shashkova, A. Wollman, S. Hohmann, M. C. Leake, Characterising Maturation of  
406 GFP and mCherry of Genomically Integrated Fusions in *Saccharomyces cerevisiae*.  
407 *Bio Protoc.* **7**, e27110 (2018).
- 408 56. H. Miller, J. Cosgrove, A. Wollman, E. Taylor, P. O’Toole, M. Coles, M. C. Leake.  
409 High-speed single-molecule tracking of CXCL13 in the B-Follicle. *Front. Immunol.*,  
410 in press (2018).
- 411 57. M. Tokunaga, N. Imamoto, K. Sakata-Sogawa, Highly inclined thin illumination  
412 enables clear single-molecule imaging in cells. *Nat. Methods*. **5**, 159–161 (2008).
- 413 58. B.-C. Chen *et al.*, Lattice light-sheet microscopy: imaging molecules to embryos at  
414 high spatiotemporal resolution. *Science*. **346**, 1257998 (2014).
- 415 59. S. Abrahamsson *et al.*, Fast multicolor 3D imaging using aberration-corrected  
416 multifocus microscopy. *Nat. Methods*. **10**, 60–63 (2013).
- 417 60. B. Yang *et al.*, High Numerical Aperture Epi-illumination Selective Plane Illumination  
418 Microscopy. *bioRxiv*, 273359 (2018).
- 419 61. K. M. Dean *et al.*, Diagonally Scanned Light-Sheet Microscopy for Fast Volumetric  
420 Imaging of Adherent Cells. *Biophys. J.* **110**, 1456–1465 (2016).
- 421 62. S. A. McKinney, C. S. Murphy, K. L. Hazelwood, M. W. Davidson, L. L. Looger, A  
422 bright and photostable photoconvertible fluorescent protein. *Nat. Methods*. **6**, 131–3  
423 (2009).
- 424 63. Z. Duan *et al.*, A three-dimensional model of the yeast genome. *Nature*. **465**, 363–7  
425 (2010).

- 426 64. H. Miller, Z. Zhou, A. J. M. Wollman, M. C. Leake, Superresolution imaging of single  
427 DNA molecules using stochastic photoblinking of minor groove and intercalating  
428 dyes. *Methods*. **88**, 81–8 (2015).
- 429 65. A. J. M. Wollman, M. C. Leake, Millisecond single-molecule localization microscopy  
430 combined with convolution analysis and automated image segmentation to determine  
431 protein concentrations in complexly structured, functional cells, one cell at a time.  
432 *Faraday Discuss.* **184**, 401–24 (2015).
- 433 66. I. Izeddin *et al.*, Single-molecule tracking in live cells reveals distinct target-search  
434 strategies of transcription factors in the nucleus. *Elife*. **3**, e02230 (2014).
- 435 67. S. A. Adam, The nuclear pore complex. *Genome Biol.* **2**, reviews0007.1-  
436 reviews0007.7 (2001).
- 437 68. C. Strambio-De-Castillia, M. Niepel, M. P. Rout, The nuclear pore complex: bridging  
438 nuclear transport and gene regulation. *Nat. Rev. Mol. Cell Biol.* **11**, 490–501 (2010).
- 439 69. W. Yang, J. Gelles, S. M. Musser, Imaging of single-molecule translocation through  
440 nuclear pore complexes. *Proc. Natl. Acad. Sci. U. S. A.* **101**, 12887–12892 (2004).
- 441 70. A. R. Lowe *et al.*, Selectivity mechanism of the nuclear pore complex characterized by  
442 single cargo tracking. *Nature*. **467**, 600–603 (2010).
- 443 71. M. A. Treitel, M. Carlson, Repression by SSN6-TUP1 is directed by MIG1, a  
444 repressor/activator protein. *Proc. Natl. Acad. Sci. U. S. A.* **92**, 3132–6 (1995).
- 445 72. Y. Phillip, G. Schreiber, Formation of protein complexes in crowded environments--  
446 from in vitro to in vivo. *FEBS Lett.* **587**, 1046–52 (2013).
- 447 73. K. Sode, S. Ochiai, N. Kobayashi, E. Usuzaka, Effect of reparation of repeat sequences  
448 in the human alpha-synuclein on fibrillation ability. *Int. J. Biol. Sci.* **3**, 1–7 (2007).
- 449 74. C. Avitabile *et al.*, Circular Dichroism studies on the interactions of antimicrobial  
450 peptides with bacterial cells. *Sci. Rep.* **4**, 337–360 (2014).
- 451 75. I. I. Cisse *et al.*, Real-Time Dynamics of RNA Polymerase II Clustering in Live  
452 Human Cells. *Science*. **341**, 664–667 (2013).
- 453 76. W.-K. Cho *et al.*, RNA Polymerase II cluster dynamics predict mRNA output in living  
454 cells. *Elife*. **5**, e13617 (2016).
- 455 77. J. Qian *et al.*, B Cell Super-Enhancers and Regulatory Clusters Recruit AID  
456 Tumorigenic Activity. *Cell*. **159**, 1524–1537 (2014).
- 457 78. M. Mir *et al.*, Dense Bicoid Hubs Accentuate Binding along the Morphogen Gradient.  
458 *Genes & Dev.* **31**, 1784–94 (2017).
- 459 79. J. Liu *et al.*, Intrinsic disorder in transcription factors. *Biochemistry*. **45**, 6873–88  
460 (2006).
- 461 80. V. N. Uversky, V. B. Patel, Intrinsically disordered proteins and their (disordered)  
462 proteomes in neurodegenerative disorders. *Front Aging Neurosci.* **7**, 18 (2015).
- 463 81. M. C. Leake, D. Wilson, M. Gautel, R. M. Simmons, The elasticity of single titin  
464 molecules using a two-bead optical tweezers assay. *Biophys. J.* **87**, 1112–35 (2004).
- 465 82. M. C. Leake, D. Wilson, B. Bullard, R. M. Simmons, The elasticity of single kettin  
466 molecules using a two-bead laser-tweezers assay. *FEBS Lett.* **535**, 55–60 (2003).



468

469 **Figure 1.** TFs form clusters in eukaryotic cell. (A) Schematic of millisecond Slimfield  
 470 microscopy. (B) Fluorescence imaging of Mig1-GFP (green) with nucleus indicated (red) by  
 471 Nrd1-mCherry, showing different cellular locations, stoichiometry determined by step-wise  
 472 photobleaching that can be measured using Fourier analysis and edge-detection filters (54,  
 473 81, 82). (C) STORM imaging using Mig1-mEos2. (D) Mobility analysis for cumulative  
 474 distribution function (CDF) and Gamma fits. (E) Mig-GFP localization through a nuclear  
 475 pore complex. (F) Dwell time for tracks translocating the nuclear envelope. (G) Images and  
 476 (H) analysis for FRAP indicating turnover of nuclear Mig1-GFP. (I) Native and denaturing  
 477 gels on purified Mig1-GFP. (J) Mig1-GFP cluster stoichiometry in presence/absence of  
 478 molecular crowding. (K) Circular dichroism spectra in presence/absence of molecular  
 479 crowding. (L) Cartoon model for shape of a Mig1 cluster in vicinity of DNA strands.





1  
2  
3  
4  
5  
6  
7  
8  
9  
10  
11  
12  
13  
14  
15  
16  
17  
18  
19  
20  
21  
22  
23  
24  
25  
26  
27  
28  
29  
30  
31  
32  
33  
34  
35  
36  
37  
38  
39  
40  
41  
42  
43  
44  
45  
46  
47  
48  
49  
50  
51  
52  
53  
54  
55  
56  
57  
58  
59  
60  
61  
62  
63  
64  
65

From: Professor Mark C. Leake FInstP, FRMS, FRSB, PhD  
Tel: +44 (0) 1904 322697/328566  
Fax: +44 (0) 1904 322214  
Email: [mark.leake@york.ac.uk](mailto:mark.leake@york.ac.uk)  
Institute: <http://www.york.ac.uk/physics/bps>  
Group: <http://single-molecule-biophysics.org>

Director, Biological Physical Sciences Institute (BPSI)  
Chair of Biological Physics  
Departments of Physics and Biology  
University of York  
Heslington  
York YO10 5DD, UK

Monday, 30 April 2018

**In reference to:** Reviewer comments for “**Transcription factors in eukaryotic cells can functionally regulate gene expression by acting in oligomeric assemblies formed from an intrinsically disordered protein phase transition enabled by molecular crowding**”

**Alberto Kornblihtt**

Dear Alberto

Many thanks for supplying the reviewer feedback: they were very helpful. I have revised the piece accordingly, and it is improved as a result. Please find overleaf a point by point response to all the reviewer comments.

If I may be of any further assistance please do not hesitate to contact me.

Yours sincerely,

Prof. Mark C. Leake

.\*\*\*



Reviewer 1:

1 Here is a small list of omitted citations on this subject that should be included to make the review more  
2 fairly  
3 balanced:

4 GR (Gebhardt, J.C. et al. <https://www.nature.com/articles/nmeth.2411>)  
5 TetR (Normanno, D. et al. <https://www.nature.com/articles/ncomms8357>)  
6 p53 (Mazza, D. et al. <https://www.ncbi.nlm.nih.gov/pmc/articles/PMC3424588/>)  
7 Sox2 (Liu Z. et al. <https://elifesciences.org/articles/04236>  
8 and  
9 Chen J. et al. <https://www.ncbi.nlm.nih.gov/pubmed/24630727>)  
10 TFIIIB  
11 (by Zhang Z. et al. <http://genesdev.cshlp.org/content/30/18/2106>)  
12  
13

14 These references have now been added  
15

16 2. The only imaging modality presented in this mini-review is Slimfield. This technique limits the  
17 observation area to a  
18 few micrometers, and hence is unsuitable to eukaryotic imaging of cells with larger nuclei. A host of  
19 other singlemolecule  
20 techniques based on light-sheet imaging have much bigger fields of view, and have the added  
21 advantage of  
22 low background and low light toxicity.  
23 Here are omitted references of imaging modalities that have been recently implemented to image  
24 eukaryotic nuclei:

25 HILO  
26 (by Tokunaga M.N. et al. <https://www.nature.com/articles/nmeth1171>)  
27 AFM cantilever lightsheet  
28 (by Gebhardt, J.C. et al. <https://www.nature.com/articles/nmeth.2411>)  
29 lattice light-sheet  
30 (by Chen B.C. et al. <http://science.sciencemag.org/content/346/6208/1257998>)  
31 multi-focus  
32 (by Abrahamsson S. et al. <https://www.nature.com/articles/nmeth.2277>)  
33 remote focusing  
34 (by Yang et al. <https://www.biorxiv.org/content/early/2018/02/28/273359>)  
35 diagonally scanned light sheet  
36 (by Dean et al. <https://doi.org/10.1016/j.bpj.2016.01.029>)  
37  
38

39 These references have now been added  
40  
41

42 3. Paragraph lines 50-64. Confusing mix of references for different model organisms: yeast, multi-  
43 cellular, and bacterial)

44 I have now clarified that these references refer to a range of different model organisms  
45  
46

47 4. Paragraph lines 114-126. The review should highlight how confinement affects apparent diffusion  
48 coefficient in the small volume of a yeast nucleus.

49 This has now been added  
50

51 5. Paragraph lines 128-144. The review should state how bleaching and dye-photophysics (blinking,  
52 dark-state transitions) are accounted for. This is especially relevant for Slimfield imaging conditions of  
53 high laser power densities.

54 Discussion has been added here concerning how blinking and bleaching dye photophysics are  
55 accounted for.  
56

57 6. Line 194: References 63 and 64 do not in fact argue for the static "transcription factories". These  
58 papers rather should be cited for time-correlated PALM (tc-PALM), which accurately accounts for dye-  
59 photophysics, and describe live cell RNA Polymerase II cluster dynamics that are quite transient.

60 This has now been added  
61  
62  
63  
64  
65

7. Lines 33-34: Eukaryotic TFs do not always fluctuate between cytoplasm and the nucleus.

This has now been corrected

8. Line 88: The author should address how <15 % fluorophore maturation is compatible with single-molecule counting.

The '<15%' refers to the immature fluorescent protein level – this has now been clarified

1  
2  
3  
4  
5  
6  
7  
8  
9  
10  
11  
12  
13  
14  
15  
16  
17  
18  
19  
20  
21  
22  
23  
24  
25  
26  
27  
28  
29  
30  
31  
32  
33  
34  
35  
36  
37  
38  
39  
40  
41  
42  
43  
44  
45  
46  
47  
48  
49  
50  
51  
52  
53  
54  
55  
56  
57  
58  
59  
60  
61  
62  
63  
64  
65